Study of Asymptotic Theory of Transonic Wind Tunnel Wall Interference

N.D. Malmuth and J.D. Cole
Rockwell International Science Center
1049 Camino Dos Rios
Thousand Oaks, CA 91360

May 1984

Final Report for Period May 30, 1982 through August 30, 1983

ARNOLD ENGINEERING DEVELOPMENT CENTER
ARNOLD AIR FORCE STATION, TENNESSEE
AIR FORCE SYSTEMS COMMAND
UNITED STATES AIR FORCE

This report has been reviewed by the Office of Public Affairs (PA) and is releasable to the National Technical Information Service (NTIS). At NTIS, it will be available to the general public, including foreign nations.
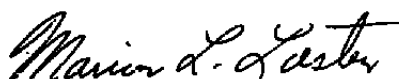
APPROVAL STATEMENT

This report has been reviewed and approved.

KEITH L. KUSHMAN
Directorate of Technology
Deputy for Operations

Approved for publication:

FOR THE COMMANDER

MARION L. LASTER
Director of Technology
Deputy for Operations

REPORT DOCUMENTATION PAGE		READ INSTRUCTIONS BEFORE COMPLETING FORM
1. REPORT NUMBER AEDC-TR-84-8	2. GOVT ACCESSION NO.	3. RECIPIENT'S CATALOG NUMBER
4. TITLE *(and Subtitle)* STUDY OF ASYMPTOTIC THEORY OF TRANSONIC WIND TUNNEL WALL INTERFERENCE		5. TYPE OF REPORT & PERIOD COVERED Final Report for Period 30 May 1982 to 30 Aug. 1983
		6. PERFORMING ORG. REPORT NUMBER SC5332.6FR
7. AUTHOR(s) N. D. Malmuth and J. D. Cole, Rockwell International Science Center		8. CONTRACT OR GRANT NUMBER(s) F40600-82-C-0005
9. PERFORMING ORGANIZATION NAME AND ADDRESS Rockwell International Science Center 1049 Camino Dos Rios Thousand Oaks, California 91360		10. PROGRAM ELEMENT, PROJECT, TASK AREA & WORK UNIT NUMBERS 65807F
11. CONTROLLING OFFICE NAME AND ADDRESS Arnold Engineering Development Center/DOS Air Force Systems Command Arnold Air Force Station, Tennessee 37389		12. REPORT DATE May 1984
		13. NUMBER OF PAGES 58
14. MONITORING AGENCY NAME & ADDRESS*(If different from Controlling Office)*		15. SECURITY CLASS. *(of this report)* Unclassified
		15a. DECLASSIFICATION/DOWNGRADING SCHEDULE N/A

16. DISTRIBUTION STATEMENT *(of this Report)*

Approved for public release; distribution unlimited.

17. DISTRIBUTION STATEMENT *(of the abstract entered in Block 20, if different from Report)*

18. SUPPLEMENTARY NOTES

Available in Defense Technical Information Center (DTIC).

19. KEY WORDS *(Continue on reverse side if necessary and identify by block number)*

transonic wind tunnels	aerodynamics
asymptotic series	fluid dynamics
transonic flow	perturbation theory
shock waves	

20. ABSTRACT *(Continue on reverse side if necessary and identify by block number)*
Asymptotic procedures have been considered for two limiting cases of wind-tunnel interference assessment on transonic models. The first corresponds to slender configurations representative of fighter aircraft, and the second is associated with high aspect ratio shapes related to bombers and transports. In the first instance, solid cylindrical walls of radius much greater than the chord lead to interference effects on the drag of a greater magnitude than the lift. A similarity law has been discovered for this effect in which the normalized drag correction is proportional to the product of the blockage ratio, and a function

DD FORM_{1 JAN 73} 1473   EDITION OF 1 NOV 65 IS OBSOLETE

20. ABSTRACT (Concluded)

of the free-stream and tunnel perturbation to the transonic similarity parameter. On the basis of this law, alterations to the similarity parameter can be sought to obtain interference-free conditions for the drag. In addition, the theory provides systematic means of extrapolating to zero model size. A numerical problem has been formulated whose solution gives the structure of the interference flow field.

For the high aspect ratio case associated with rectangular cross-section solid walls, asymptotic methods give a framework which is a generalization of lifting line theory for unconfined flows. Near the wing, the flow retains the two-dimensional strip theory character of the free-field situation. By contrast, the far field consists of a bound vortex, shedding trailing vorticity at a rate proportional to the spanwise gradient in the spanwise load distribution. The bound vortex is perpendicular to the flow and in the plane of the wing. Both the bound and shed elements are reflected in the walls. The induction of this vortex assemblage modifies the incidence of the span elements in the near-field strip theory. A Green's function has been developed expressing the potential of the assemblage, and matching procedures are outlined to calculate the nonlinear interaction of the near and far fields.

PREFACE

This report constitutes the final report of Air Force contract F40600-82-C-0005, Study of Asymptotic Theory of Transonic Wind Tunnel Wall Interference. This effort was conducted under the sponsorship of Arnold Engineering Development Center, (AEDC), Air Force Systems Command (AFSC), Arnold Air Force Station, Tennessee 37389. Dr. Keith Kushman was the AEDC technical representative for the contract. The manuscript was sumbitted for publication on May 8, 1984. The reproducibles used in the reproduction of this report were supplied by the authors.

CONTENTS

CONTENTS (Continued)

ILLUSTRATIONS

Figure

APPENDICES

1.0 INTRODUCTION

The problem of obtaining free-field transonic characteristics of wind tunnel models will continue to be of central importance to aeronautical technology for the indefinite future. Although the wind tunnel interference problem has received considerable attention at subsonic speeds, and a number of classical theories have been developed, e.g., Refs. 1-3, there is room for progress even in this linear regime, as exemplified by the recent efforts of Kraft[4], who devised an ingenious procedure based on Cauchy's integral formula for two-dimensional flow over confined airfoils. This method has been extended to the three-dimensional flow by Sickles and Kraft in Ref. 5. Among its advantages, in contrast to the older concepts, is that by measurement of two flow variables it eliminates the need for both knowledge of the wall characteristics and analytical synthesis of the model. Presently, effort is underway to extend this procedure to nonlinear transonic flows.

In connection with the transonic regime, other procedures have been developed which possess attractive features. One, which is of great interest, is a scheme that has been developed by Murman. This "post test assessment method", which has been implemented in two dimensions in Ref. 6, is similar in some respects to an approach developed earlier by Kemp[7], and assumes a knowledge of the experimental pressures on the model and walls. It uses modern computational and optimization procedures to determine whether the tunnel Mach number and model angle of attack are correctable in the sense that almost free-field model pressures can be obtained at practically altered values of these parameters. For this purpose, an inverse problem needs to be solved. In three dimensions, surface pressures over the model are generally not available, and efforts are currently underway to modify the method toward the use of less information regarding the model near field. Examples of schemes of this kind are given in Refs. 5, 8, and 9. If this goal can be achieved, this process will be of value, including treatment of cases in which the walls are relatively close to the model. In spite of the potential utility of this method, there is a need for approaches that can reduce the

number of input parameters necessary to compute the correction, shed light on the physics of the wall interference phenomena, simplify the necessary computations, and be generalized to three dimensions, as well as unsteady flows. Asymptotic procedures provide such advantages. Furthermore, they can provide valuable interactions with the other methods previously mentioned to suggest possible improvements as well as deriving beneficial features from them as well. For example, one concept presently being considered in the simplification of the Murman method of Ref. 6 for three-dimensional applications is unfolding a singular character of the near field rather than obtaining the model's shape from an inverse solution of a problem involving specified pressures based on measured values. In Ref. 10, an asymptotic procedure for two-dimensional transonic flow was developed. From this analysis, the singular character can be obtained from certain limit processes. Moreover, nonlinear integral theorems as well as the asymptotic structure of nonlinear integral equations arising in the matching scheme occurring in the asymptotic analysis could be of use in the procedure of Refs. 4 and 5.

Other potential applications of the asymptotic theory involve adaptive wind tunnels. An example of one configuration is described in Ref. 11.

The analysis given herein will be oriented toward the three-dimensional generalization of asymptotic solutions developed for the two-dimensional case in Ref. 10. The latter represent the application of perturbation theory to the solid wall interference problem at transonic speeds. Whereas many of the previous methods can handle arbitrary wall to model dimension ratios, h, the perturbation procedure assumes h to be large. This approximation is useful for many practical cases in which it is desired to minimize the wall interference. Furthermore, even for situations where h is not so large, the expansions appear to have extended validity.

A previous analysis along these lines was conducted by Chan[12], who treated the two-dimensional porous wall case based on asymptotic developments similar to those given for transonic lifting line theory in Ref. 13. Because of its interest in connection with compliant boundary applications and the fact that the Chan solutions apparently do not subsume it, we have analyzed the solid wall case. By contrast to the method of Ref. 12, we employ

"intermediate variables" to match the model near and far fields. Although slightly more cumbersome than the approach utilized by Van Dyke[14], it provides a reliable means of ensuring that all the proper terms are included in both representations.

In addition, numerical solutions have been obtained for this theory, as typified in Ref. 10, to give some insight into the nature and magnitude of the interference effects. The work of Ref. 12 in this sense was strictly formulational, with no computational application or quantification of the interference given.

This report provides three-dimensional generalizations of the two-dimensional theory of Ref. 10. The development of these models was conducted under Air Force Contract F40600-82-C0005 and monitored at Arnold Engineering Development Center. The program consisted of the following two tasks:

Task 1. Asymptotic procedures will be considered for two limiting cases: slender configurations representative of fighter aircraft, and high aspect ratio configurations representative of transports. The feasibility and general approach of applying asymptotic theory to these cases will be determined.

Task 2. Based on the results of Task 1 and following consultation with the sponsor of the work, either the slender or high aspect ratio case will be selected for development of the theory for assessment/ correction of wall interference for three-dimensional transonic flow.

On the basis of Task 1, the low aspect ratio received emphasis in this program. Within this framework, the case of a slender fighter vehicle confined within cylindrical wind tunnel walls was treated. The corresponding theory described herein provides the formulation of a numerical problem whose solution* gives the wall-induced interference correction. Although the results apply to sting-mounted models confined by cylindrical solid walls, they can be readily extended to other support arrangements and wall cross sections. These

---

*To be obtained in future contract effort.

generalizations simplify the numerical work required for the assessment/correction as compared to purely computational schemes. Porous and slotted, as well as other boundary conditions such as a specified pressure distribution on a control surface for interference assessment, and adaptive applications can also be handled. The theory applies to the situation when the characteristic lateral dimension of the model is small compared to its length, and the tunnel height is inversely proportional to this lateral dimension. To be provided in this report is information from the theory on the forces and pressures associated with the interference.

In another phase of the effort, progress has been made in the development of a comparable model for confined high aspect ratio shapes. Basic ideas have been worked out which represent a generalization of transonic lifting line theory. Means have been identified which will be helpful in matching the vortex sheet far field representation consisting of a lifting line reflected in the walls with the nonlinear almost two-dimensional near field. These developments will be summarized in what follows. On the basis of this effort, recommendations for future study will be made.

2.0 ANALYSES

2.1 CONFINED SLENDER CONFIGURATIONS

2.1.1 <u>Overview and Roadmap</u>

In what follows, a slender confined airplane model shown schematically in Fig. 1 will be considered. The flow structure consists of three zones in which different approximations for the perturbation potential apply. These regions are indicated in Fig. 2. Near the axis of symmetry of an equivalent body of revolution having the same streamwise distribution of cross-sectional area as the complete airplane (axis layer), lateral gradients dominate. In a "central layer", if α, the angle of attack, and the characteristic thickness, δ, are such that $\alpha/\delta = O(1)$, as $\delta \to 0$, the flow is nearly axisymmetric and can be characterized as a nonlinear line source. Asymptotic representations for the central and axis layers exist in which the first order terms are those associated with the unconfined flow. The
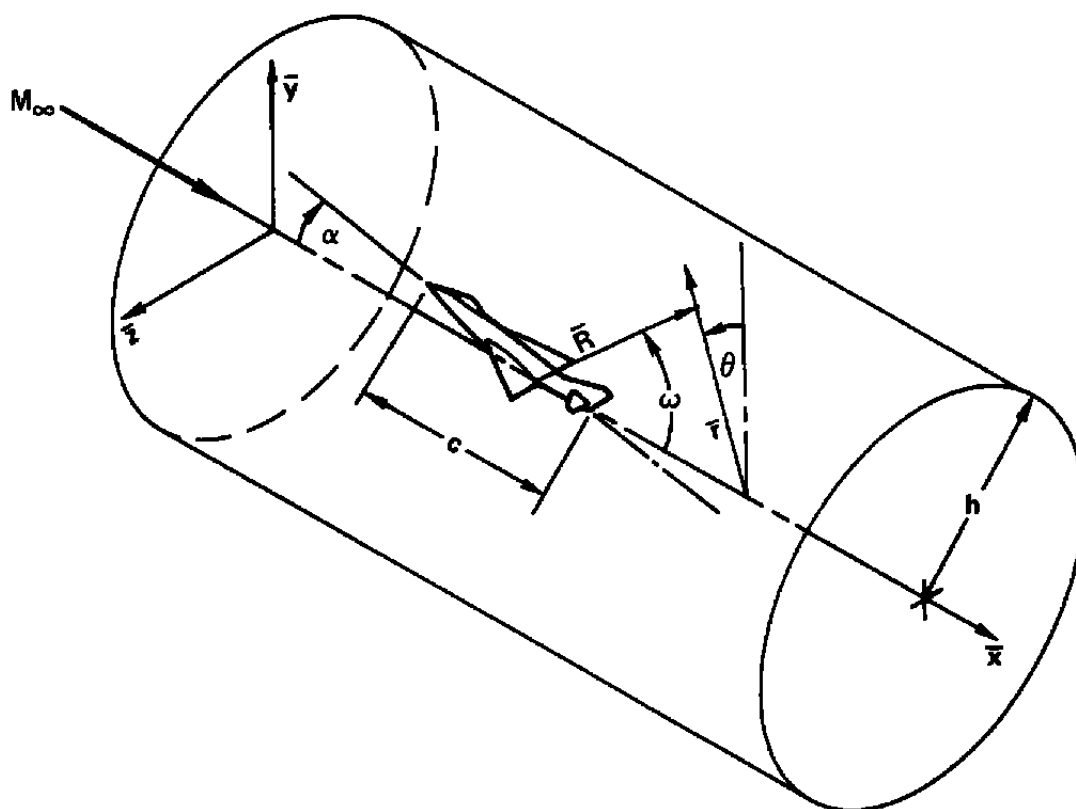
Fig. 1   Slender vehicle confined inside cylindrical wind
tunnel walls indicating Cartesian, cylindrical, and
spherical polar coordinates used in analysis.
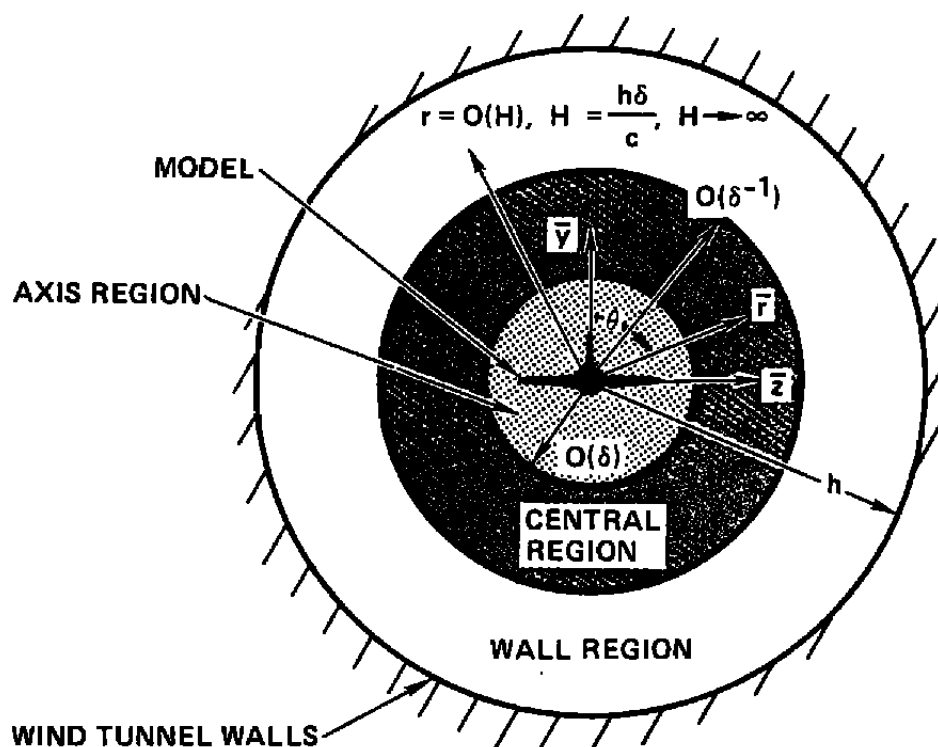
Fig. 2 Front view of wind tunnel model confined by cylindrical
walls, showing regions of applicability of asymptotic
expansions.

second order corrections of these regions are due to the wall effects. A third
region denoted as the wall layer can be identified, where the assumption of
small wall perturbations is invalid. Here, other simplifications apply which
represent the slender airplane as a multipole reflected in the walls.

*The effect of the walls on the flow field is deduced by solving the
second order problem for the central layer. This consists of the equation
of motion, hereinafter referred to as the "variational equation", subject
to boundary conditions devised from matching the wall and axis layers.*

Besides furnishing boundary conditions, the matching process is used to determine unknown elements appearing in each of the representations for the various layers. It consists of comparing these representations in a common region to two of them.

In what follows, details of the matching process will be provided. Once the asymptotic form of the solution is determined, it will be used to evaluate the influence of the walls on the pressures and forces on the confined body.

2.1.2 Mathematical Details

Karman-Guderley Approximation

The flow over a slender airplane wind tunnel model shown in Fig. 1 is considered in which the surface of the test article is given by

$$r = \delta F(x,\theta) , \tag{1}$$

in cylindrical coordinates. In the notation of Fig. 1, normalized coordinates,

$$x = \frac{\bar{x}}{c} , \quad r = \frac{\bar{r}}{c} , \tag{2}$$

(in which c is a characteristic body length) are introduced, and the bars signify dimensional quantities.

The Karman-Guderley (KG) representation of the velocity potential in small disturbance theory is given by the following asymptotic expansion:

$$\frac{\Phi}{U} = \bar{x} + \delta^2 \phi(x,\tilde{r},\theta;K,H,A) + \cdots , \tag{3}$$

which is an approximate representation of Φ in the KG limit,

$$x,\tilde{r} = \delta r,\theta \quad , \quad K = \frac{1-M_\infty^2}{\delta^2} \quad , \quad H = \frac{h\delta}{c} \quad , \quad A = \frac{\alpha}{\delta} \text{ fixed} \quad , \text{ as } \delta \to 0 . \tag{4}$$

Central Layer Expansion

Within the KG limit, secondary limits involving $H \to \infty$ can be considered*. For slender airplane models confined by wind tunnel walls, various regions can be identified in which approximations for the perturbation potential ϕ hold. These approximations are expressed as asymptotic expansions. In the central region depicted in Fig. 2 (away from the $\bar{x}$ axis and the walls), the perturbation potential ϕ is almost axisymmetric and has the representation

$$\phi = \phi_0(x,\tilde{r}) + \mu_{\frac{1}{2}}(H)\phi_{\frac{1}{2}} + \mu_1(H)\phi_1 + \cdots \tag{5a}$$

which holds in the central region limit

$$x, \tilde{r} \text{ fixed as } H \to \infty, \tag{5b}$$

where the quantity $\mu_{\frac{1}{2}}(H)\phi_{\frac{1}{2}}$ is a "switchback" term inserted for matching.

For purposes of studying the possibility of obtaining interference-free conditions, the KG similarity parameters K and A can also be expressed in the perturbation forms

$$K = K_0 + \nu_1(H)K_1 + \cdots \tag{5c}$$

$$A = A_0 + \kappa_1(H)A_1 + \cdots . \tag{5d}$$

In (5a), (5c), and (5d), the flow quantities are small perturbations about their free field (subscript 0) values consistent with $H \to \infty$. In what follows, only (5c) will be considered to obtain values of K_1 for interference-free loading on the model.

---

*The approximation scheme contrasts with another one which is embedded in a full potential framework under development by the authors.

On substitution into the KG equations and retaining like order terms, (5a) and (5c) lead to the following equations for the secondary approximations ϕ_0, $\phi_{\frac{1}{2}}$, and ϕ_1:

$$\left[K_0 - (\gamma+1)\phi_{0_x}\right]\phi_{0_{xx}} + \frac{1}{\tilde{r}}\left(\tilde{r}\phi_{0_{\tilde{r}}}\right)_{\tilde{r}} = 0 \tag{6a}$$

$$\left[K_0 - (\gamma+1)\phi_{0_x}\right]\phi_{\frac{1}{2}_x} - (\gamma+1)\phi_{0_{xx}}\phi_{\frac{1}{2}_x} + \frac{1}{\tilde{r}}\left(\tilde{r}\phi_{\frac{1}{2}_{\tilde{r}}}\right)_{\tilde{r}} = 0 \tag{6b}$$

$$\left[K_0 - (\gamma+1)\phi_{0_x}\right]\phi_{1_{xx}} - (\gamma+1)\phi_{1_x}\phi_{0_{xx}} + \frac{1}{\tilde{r}}\left(\tilde{r}\phi_{1_{\tilde{r}}}\right)_{\tilde{r}} = -K_1\phi_{0_{xx}} \ . \tag{6c}$$

The forcing term in (6c) is necessary to achieve interference-free flow conditions. Its retention requires that

$$\nu_1(H) = \mu_1(H) \ . \tag{7}$$

For matching, a procedure described in Appendix A based on Green's theorem gives a far field representation for ϕ_0 for a "ray" limit in which

$$\underline{R} = \sqrt{x^2 + K_0\tilde{r}^2} \to \infty \quad , \quad \omega = \cos^{-1}\frac{x}{\underline{R}} \text{ fixed} \ , \tag{8a}$$

where

$$R = \underline{R}/\sqrt{K_0} = \sqrt{X^2 + \tilde{r}^2} \quad , \quad X = x/\sqrt{K_0} \ . \tag{8b}$$

From this process, the far field representation is

$$\phi_0 = \frac{A_0}{\underline{R}} + \frac{B_0}{\underline{R}^2} \cos\omega + \frac{C_0}{\underline{R}^3} \left(\cos3\omega + \frac{2}{5}\cos\omega\right) + \frac{A}{\underline{R}^3} P_2(\cos\omega) + 0\left(\frac{\ell n\ \underline{R}}{\underline{R}^4}\right) , \qquad (9a)$$

where $P_n(\cos\omega)$ is a Legendre polynomial and

$$\underline{A}_0 = -\frac{S(1)}{4\pi} , \quad 4\pi\underline{B}_0 = -S(1) + \int_0^1 S(x)dx + \frac{\pi(\gamma+1)}{K_0} \int_{-\infty}^{\infty}dx\int_0^{\infty} \tilde{r}\phi_0^2{}_x(x,\tilde{r})d\tilde{r} ,$$

$$\underline{C}_0 = \frac{S^2(1)(\gamma+1)}{16\pi^2 K_0} \qquad (9b)$$

$$S(x) = \frac{1}{2}\int_0^{2\pi} F^2 d\theta . \qquad (9c)$$

The constant $\underline{A}$ has not been determined and will not require an evaluation in what follows.

Wall Layer Expansion

The central region expansions (5a), (5c), and (5d) are nonuniformly valid at the walls. This is associated with the idea that the wall induced perturbations are no longer small in that domain. Instead, the appropriate representation is:

$$\phi = \epsilon_0(H)\varphi_0(x^\dagger,r^\dagger) + \epsilon_1(H)\varphi_1(x^\dagger,r^\dagger) + \cdots \qquad (10)$$

which is valid in the wall layer limit

$$x^\dagger = \frac{x}{H} , \quad r^\dagger = \frac{\tilde{r}}{H} , \quad \text{fixed as } H \rightarrow \infty .$$

By the substitution procedure previously described, the wall layer approximation can be shown to satisfy the following hierarchy:

$$K_0 \varphi_{0_{x^+ x^+}} + \frac{1}{r^+}\left(r^+ \varphi_{0_{r^+}}\right)_{r^+} = 0 \tag{11a}$$

$$K_0 \varphi_{1_{x^+ x^+}} + \frac{1}{r^+}\left(r^+ \varphi_{1_{r^+}}\right)_{r^+} = -K_1 \varphi_{0_{x^+ x^+}} + (\gamma+1)\varphi_{0_{x^+}}\varphi_{0_{x^+ x^+}} \tag{11b}$$

and

$$\left.\frac{\partial \varphi_i}{\partial r^+}\right|_{r^+=1} = 0 \quad , \quad i=1,2,\cdots . \tag{11c}$$

Integral Representation for φ_0

If $S(1) \neq 0$, as for the case of a sting support rather than a magnetic suspension*, φ_0 must behave as a reflected source near the origin $R^+ = 0$ in order to match with the dominant term of ϕ_0 given in (9a). From Appendix B, the appropriate solution with this property can be derived to be

$$\varphi_0 = \frac{S(1)}{\sqrt{K_0}}\left\{\frac{X^+}{2\pi}\operatorname{sgn} X^+ + M\right\} , \tag{12a}$$

where

$$X^+ = x^+/\sqrt{K_0} \tag{12b}$$

$$M = M_0 + M_1 \tag{12c}$$

---

*This analysis can be extended to treat the magnetic suspension case.

$$M_0 = -\frac{1}{2\pi^2} \int_0^\infty \cos kX^\dagger K_0(kr^\dagger) dk \tag{12d}$$

$$M_1 = \frac{1}{\pi} \int_0^\infty \cos kX^\dagger \left\{ \frac{1}{\pi k^2} - \frac{K_1(k) I_0(kr^\dagger)}{2\pi I_1(k)} \right\} dk \ , \tag{12e}$$

and I_n and K_n are modified Bessel functions of order n.

φ_0 Asymptotics for Small $R^\dagger$

For matching, the behavior of φ_0 for $R^\dagger = R/H \rightarrow 0$, ω fixed, is needed. In this connection, the representations (12d) and (12e) can be expanded near the origin by Taylor's theorem or another method involving differentiation with respect to $r^\dagger$ and $X^\dagger$ described in Appendix C. This process gives

$$\varphi_0 = \frac{S(1)}{\sqrt{K_0}} \left\{ -\frac{1}{4\pi R^\dagger} + a_0 + b_0 R^{\dagger^2} P_2(\cos\omega) + \cdots \right\} \ , \tag{13a}$$

where*

$$a_0 = \frac{1}{\pi^2} \int_0^\infty \left\{ \frac{1}{k^2} - \frac{K_1(k)}{2I_1(k)} \right\} dk \tag{13b}$$

$$b_0 = \frac{1}{4\pi^2} \int_0^\infty \frac{k^2 K_1(k)}{I_1(k)} dk \ . \tag{13c}$$

The integrals in (13b) and (13c) are convergent, can be evaluated once and for all numerically, and are independent of $X^\dagger$ and $r^\dagger$.

---

*Similar quadratic growth to the $R^{\dagger^2}$ term occurs in the two-dimensional case.

Matching of Central and Wall Layers

An intermediate variable and limit are introduced such that

$$R_\eta = \frac{R}{\eta(H)} \quad , \quad \omega \text{ fixed as } H \to \infty \ . \tag{14}$$

Here, $\eta(H)$ is of an order between unity and H. This property is expressed symbolically as

$$1 \ll \eta(H) \ll H \ . \tag{15}$$

The central region representation for ϕ in the intermediate limit (14) is

$$\phi = \underbrace{\frac{A_0}{\eta R_\eta}}_{①} + \underbrace{\frac{B_0}{\eta^2 R_\eta^2} \cos\omega}_{②} + \underbrace{\frac{C_0}{\eta^3 R_\eta^3} \left\{\cos 3\omega + \frac{2}{5} \cos\omega\right\} + \frac{A}{\sqrt{K_0}\,\eta^3 R^3} P_2(\cos\omega)}_{③}$$

$$+ \underbrace{0\left(\frac{\ell n \eta R_\eta}{\eta^4 R_\eta^4}\right)}_{④} + \underbrace{\mu_{\frac{1}{2}}(H)\phi_{\frac{1}{2}}}_{⑤} + \underbrace{\mu_1(H)\phi_1(R_\eta,\omega)}_{⑥} \tag{16}$$

where

$$A_0 = \underline{A_0}/\sqrt{K_0} \quad , \quad B_0 = \underline{B_0}/\sqrt{K_0} \quad , \quad C_0 = \underline{C_0}/\sqrt{K_0} \ .$$

The central and wall layer representations for ϕ have an "overlap" domain of common validity as can be demonstrated by writing the wall layer representation in the intermediate limit (14). This gives

$$\phi = \varepsilon_0(H) \frac{S(1)}{\sqrt{K_0}} \left\{ - \frac{1}{4\pi \frac{\eta}{H} R_\eta} + a_0 + b_0 \frac{\eta^2}{H^2} R_\eta^2 P_2(\cos\omega) + \cdots \right\} + \varepsilon_{\frac{1}{2}} \varphi_{\frac{1}{2}} \left(\frac{\eta}{H} R_\eta, \omega \right)$$

$$\textcircled{1}' \qquad \textcircled{2}' \qquad \textcircled{3}' \qquad \textcircled{4}'$$

$$+ \varepsilon_1(H) \varphi_1 \left(\frac{\eta}{H} R_\eta, \omega \right) + \cdots . \tag{17}$$

$$\textcircled{5}'$$

where an additional switchback term $\textcircled{4}'$ has been inserted in (10) to match $\textcircled{2}$. Upon identifying common terms, denoted below by $\leftrightarrow$, matching demands that the following identities hold:

$$\underline{\textcircled{1} \leftrightarrow \textcircled{1}'}$$

$$\varepsilon_0 = 1/H \tag{18a}$$

$$A_0 = - \frac{1}{4\pi} \frac{S(1)}{\sqrt{K_0}} \tag{18b}$$

$$\underline{\textcircled{3} \leftrightarrow \textcircled{5}'}$$

$$\varepsilon_1(H) = 1/H^3 \tag{19a}$$

$$\varphi_1 \simeq R^{+-3} \left\{ C_0 \left(\cos 3\omega + \frac{2}{5} \cos\omega \right) + \frac{\underline{A}}{\sqrt{K_0}} P_2(\cos\omega) \right\} - \frac{4\pi b_0}{\sqrt{K_0}} \underline{A}$$

$$\text{as } R^+ \to 0 . \tag{19b}$$

Equation (19b) is consistent with the fact that the terms on the right hand side are solutions of (11b) which is to dominant order identical in form to (6c). These terms are particular and homogeneous solutions identified in (9a). For φ_1, the homogeneous solution can be obtained from differentiation with respect to X of the switchback term $\varphi_{\frac{1}{2}}$ and adjusting the quadrupole strength for matching. The quantity $\varphi_{\frac{1}{2}}$ itself is obtained from differentiation of φ_0 with respect to X. It satisfies an equation identical to (11a) and can be shown to be $\simeq B_0 \cos\omega \left| R^{+-2} + 8\pi b_0 R^+ \right|$ as $R^+ \to 0$.

(6) ↔ (3')

$$\mu_1(H) = 1/H^3 \tag{20a}$$

$$\phi_1 = b_0 \left[\frac{S(1)}{\sqrt{K_0}} R^2 P_2(\cos\omega) + 8\pi B_0 R \cos\omega - \frac{4\pi A}{\sqrt{K_0}} \right] \text{ as } R \to \infty . \tag{20b}$$

In the formulation of the numerical problem for ϕ_1, the last term in (20b) will be neglected in the far field specification.

(2') ↔ (5)

$$\mu_{\frac{1}{2}} = 1/H \tag{21a}$$

$$\phi_{\frac{1}{2}} = a_0' = \frac{S(1)}{\sqrt{K_0}} a_0 , \tag{21b}$$

noting that (6b) is identically satisfied by the constant a_0'.

Axis Layer Expansion

The third region of importance is a zone near the x axis shown in Fig. 2 and denoted as the axis layer. In this region, as in the unconfined case, cross flow gradients dominate. This is related to the fact that the scale of the r gradients in this domain is δ. The asymptotic representation for the velocity potential is

$$\frac{\phi}{U} = \bar{x} + c[2(\delta^2 \ln\delta)\mathscr{P}^*(x) + \delta^2 \phi^*(x, r^*, \theta, K, H, A) + \cdots] \tag{22a}$$

which is valid in the axis limit

$$r^* = r/\delta, K, H, A \quad \text{fixed as } \delta \to 0 . \tag{22b}$$

Here, r and θ are cylindrical coordinates shown in Fig. 2.

As a representation of the wall effects, the perturbation potential, ϕ^*, has the development

$$\phi^* = \phi_0^* + \tau_{\frac{1}{2}}(H)\phi_{\frac{1}{2}}^* + \tau_1(H)\phi_1^* + \cdots \tag{23a}$$

which holds in the limit

$$r^*, K, A \quad \text{fixed as } \delta \to 0, \; H \to \infty \text{ independently .} \tag{23b}$$

In (23a), the quantity involving $\tau_{\frac{1}{2}}$ is a switchback term inserted to match with its counterpart involving $\mu_{\frac{1}{2}}$ in (5a).

Problems for ϕ_0^*, $\phi_{\frac{1}{2}}^*$, and ϕ_1^*

On substitution of (23a) into exact equations and boundary conditions, the boundary value problems satisfied by ϕ_0^*, $\phi_{\frac{1}{2}}^*$, and ϕ_1^* in (23a) can be determined.

For ϕ_0^*,

$$\Delta\phi_0^* \equiv \frac{1}{r^*} \cdot \frac{\partial}{\partial r^*}\left(\frac{r^* \partial \phi_0^*}{\partial r^*}\right) + \frac{1}{r^{*2}} \frac{\partial^2 \phi_0^*}{\partial \theta^2} = 0 \tag{24a}$$

holds in the region external to the cross flow boundary $B = 0$ shown in Fig. 3. This boundary is the projection of the model shown in Fig. 1 in a plane perpendicular to the free stream. Equation (24) is solved subject to the flow tangency condition on the boundary.

$$\left.\frac{\partial \phi_0^*}{\partial n}\right|_B = \frac{FF_x}{F^2 + F_\theta^2} , \tag{24b}$$

where n signifies differentiation in the normal direction to the surface $B = r^* - F(x,\theta) = 0$, and B signifies evaluation of this derivative on the surface.
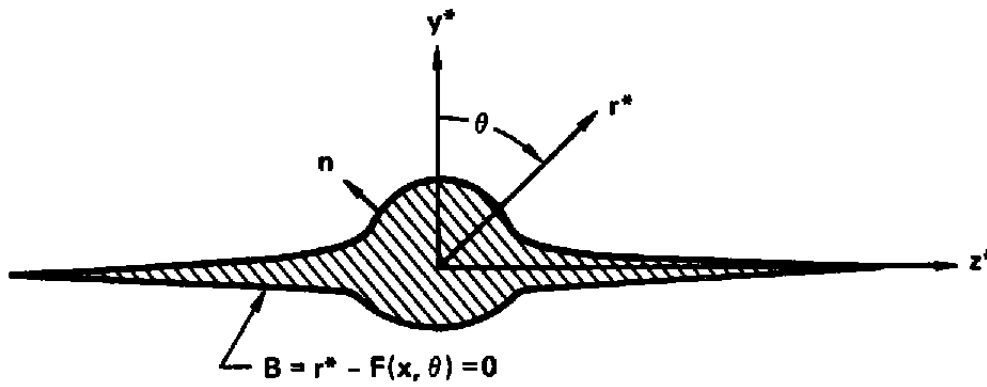
Fig. 3 Cross flow plane geometry.

On the basis of Gauss' divergence theorem and (24b),

$$\phi_0^* \simeq \frac{S'(x)}{2\pi} \ln r^* \quad \text{as } r^* \to \infty .$$ (24)

The problems for the other quantities are

$$\Delta\phi_{\frac{1}{2}}^* = \Delta\phi_1^* = 0$$ (25a)

$$\left.\frac{\partial\phi_{\frac{1}{2}}^*}{\partial n}\right|_B = \left.\frac{\partial\phi_1^*}{\partial n}\right|_B = 0 .$$ (25b)

By matching considerations, it is anticipated that

$$\phi_{\frac{1}{2}}^*, \phi_1^* < \infty \quad \text{as } r^* \to \infty .$$ (25c)

Solutions for Axis Layer Approximations

On the basis of Eqs. (24) and (25), the following multipole representations hold:

$$\phi_0^* = \frac{S'(x)}{2\pi} \ln r^* + g_0^{*(0)}(x) + \sum_{n=1}^{\infty} \frac{g_n^{*(0)}(x)\cos n\theta}{r^{*n}} \qquad (26a)$$

$$\phi_{\frac{1}{2}}^* = \text{constant} = C_1 \qquad (26b)$$

$$\phi_1^* = g_0^{*(1)}(x) \ , \qquad (26c)$$

where without loss of generalization, lateral symmetry has been assumed in the sense that $F(x,\theta) = F(x,-\theta)$.

Matching of Axis and Central Layers

Following a procedure similar to that employed in the subsection relevant to Central-Wall Layer matching, a suitable intermediate variable is introduced. For the overlap domain of common validity of the axis and central layers, this variable is assumed to be

$$r_\zeta = \frac{r}{\zeta(\delta)} \qquad (27)$$

where

$$\delta \ll \zeta(\delta) \ll \delta^{-1} \ . \qquad (28)$$

The axis layer representation for Φ written in intermediate variables is then

$$\frac{\Phi}{U} = x + 2(\delta^2 \ln\delta)\mathscr{P}^*(x) + \delta^2 \left\{ \left[\ln\zeta r_\zeta - \ln\delta \right] \mathscr{P}^*(x) + g_0^{*(0)}(x) \right.$$

①   ② ③ ④

$$\left. + \tau_{\frac{1}{2}} C_1 + \tau_1 \left[g_0^{*(1)}(x) + \cdots \right] \right\} . \tag{29}$$

⑤ ⑥

$$\mathscr{P}^* \equiv S'(x)/2\pi .$$

For the central layer, the corresponding representation is

$$\frac{\Phi}{U} = x + \delta^2 \left\{ \mathscr{P}(x) \left[\ln\delta + \ln\zeta r_\zeta \right] + g_0(x) + \frac{a_0'}{H} + \frac{1}{H^3} g_1(x) + \cdots \right\} . \tag{30}$$

①′ ②′ ③′ ④′ ⑤′

On the basis of (29) and (30), the following matchings apply:

① + ③ ↔ ①′

$$\mathscr{P}^*(x) = \frac{S'(x)}{2\pi} = \mathscr{P}(x) \tag{31}$$

② ↔ ②′

Already matched.

④ ↔ ③′

$$g_0^{*(0)}(x) = g_0(x) \tag{32}$$

$\textcircled{5} \leftrightarrow \textcircled{4'}$

$$\tau_{1_{\frac{1}{2}}} = 1/H \tag{33a}$$

$$C = a_0^{\prime} \tag{33b}$$

$\textcircled{6} \leftrightarrow \textcircled{5'}$

$$\tau_1 = 1/H^3 \tag{34}$$

$$g_0^{*(1)} = g_1(x) \ . \tag{35}$$

This completes the matching process.

Summary of Representations for Potentials in Various Regions

Collecting the previous results, the asymptotic expansions for the velocity potential in the Axis, Central, and Wall layers are

Axis Layer

$$\frac{\Phi}{U} = x + \frac{1}{\pi}(\delta^2 \ell n \delta) S'(x) + \delta^2 \left\{ \phi_0^*(x,r^*) + \frac{a_0^{\prime}}{H} + \frac{g_1(x)}{H^3} + \cdots \right\} \ , \tag{36}$$

$$r^* = r/\delta$$

Central Layer

$$\frac{\Phi}{U} = x + \delta^2 \left\{ \phi_0(x,\tilde{r}) + \frac{a_0^{\prime}}{H} + \frac{1}{H^3} \phi_1(x,\tilde{r}) + \cdots \right\} \ , \tag{37}$$

$$\tilde{r} = \delta r$$

Wall Layer

$$\frac{\Phi}{U} = x + \delta^2 \left\{ \frac{1}{H} \varphi_0(x^\dagger, r^\dagger)^{\cdot} + \frac{1}{H^2} \varphi_{\frac{1}{2}}(x^\dagger, r^\dagger) + \frac{1}{H^3} \varphi_1(x^\dagger, r^\dagger) + \cdots \right\} , \quad (38)$$

$$x^\dagger = \frac{x}{H} \quad , \quad r^\dagger = \frac{\tilde{r}}{H} ,$$

$$a_0^{\prime} \equiv \frac{S(1)}{\pi^2 \sqrt{K_0}} \int_0^\infty \left\{ \frac{1}{k^2} - \frac{K_1(k)}{2I_1(k)} \right\} dk .$$

Associated with obtaining interference-free loadings, the KG similarity parameter has the expansion

$$K = K_0 + \frac{1}{H^3} K_1 + \cdots . \quad (39)$$

Interference Pressure Distribution on the Model

On the basis of Ref. 15, the pressure distribution C_{P_B} on the model is

$$\frac{C_{P_B}}{\delta^2} = -\frac{1}{2\pi} (\delta^2 \, \ell n \delta) S''(x) - 2\phi_x^* \Big|_B + v_B^{*2} + w_B^{*2} \quad (40)$$

where

$$v_B^* = \frac{\partial \phi^*}{\partial r^*} \Big|_{r^*=F} \quad , \quad w_B^* = \frac{1}{r^*} \frac{\partial \phi^*}{\partial \theta} \Big|_{r^*=F} \quad , \quad \Big|_B \equiv \Big|_{r^*=F} .$$

Substituting (36) in (40), this pressure can be written as

$$\frac{C_{P_B}}{\delta^2} = -\frac{1}{2\pi} (\delta^2 \, \ell n \delta) S''(x) - 2 \left\{ \phi_{0_x}^* \Big|_B + \frac{g_1^{\cdot}(x)}{H^3} \right\} + \left(\frac{\partial \phi_0^*}{\partial r^*} \right)^2 \Big|_B + \left(\frac{1}{r^*} \frac{\partial \phi_0^*}{\partial \theta} \right)^2 \Big|_B . \quad (41)$$

Hence, the wall interference effect on the surface pressures denoted as ΔC_p is independent of θ and is given by

$$\Delta C_p = -\frac{2\delta^2}{H^3} g_1'(x) \ . \tag{42}$$

From (41) and (42), the loading on the model is constant in each streamwise plane $x = $ constant. Accordingly, the walls induce no lift perturbation on the model. Only a drag perturbation occurs. This is considered in the next section.

Tunnel-Wall Interference Drag

The drag D of the wind-tunnel model can be computed by applying the analysis of Ref. 15, which was performed for unconfined flows. Therein, D is computed from a momentum flux in the x direction across the boundaries of a cylindrical control surface. The curved boundaries of this surface coincide with those of the Axis Layer. From this procedure, D in an unconfined flow is given as

$$\frac{D}{2q} + \delta^4 \ln\delta\left[2\pi\mathscr{S}^2(1)\right] = \delta^4\left\{\pi\mathscr{S}(1)g(1) - \frac{1}{2}\int_0^{2\pi}\phi^*(1,F,\theta)FF_x(1,\theta)d\theta \right.$$

$$\left. - 2\pi\int_0^1 \mathscr{S}(x)g'(x)dx\right\}. \tag{43}$$

In (43),

$$g(x) = \lim_{\tilde{r}\to 0}\left\{\phi - \mathscr{S}(x)\ln\tilde{r}\right\} \tag{44}$$

$q = $ dynamic pressure .

The wall induced perturbation to the drag ΔD is computed from the change in ϕ^* due to the second and third order terms, using (43) whose structure is otherwise unaffected by the walls. The result is

$$\frac{\Delta D}{q} = \frac{2\delta^4}{H^3} \int_0^1 S'(x)g_1'(x)dx \ .$$

$$(45)$$

Since S is proportional to δ^{-2} multiplied by the unscaled cross sectional area, the change in drag coefficient normalized to the product of the model frontal area and $\frac{1}{H}$, $H\Delta C_D$ is proportional to δ^2/H^2. This quantity is in turn proportional to the blockage ratio, a_r, i.e., δ^2/h^2.

Determination of Interference-Free Conditions for Drag

For a given model geometry or an affinity of models, Eq. (45) can be written in the form

$$\frac{H\Delta C_D}{a_r} = f(K_0, K_1, A, \gamma) \ .$$

$$(46)$$

This relation is a similarity law in which H, a_r are separated out of the universal variation given by f. The latter is determined solely from (45) through g_1. To determine this quantity, the following boundary value problem (P1) needs to be solved for the previously given variational equation for ϕ_1.

P1:

$$\left[K_0 - (\gamma+1)\phi_{0_x}\right]\phi_{1_{xx}} - (\gamma+1)\phi_{0_{xx}}\phi_{1_x} + \frac{1}{\tilde{r}}\left(\tilde{r}\phi_{1_{\tilde{r}}}\right)_{\tilde{r}} = -K_1\phi_{0_{xx}} \qquad (6c)$$

$$\lim_{\tilde{r} \to 0} \phi_{1_{\tilde{r}}} = 0 \qquad (47)$$

$$\phi_1 \simeq b_0' R^2 P_2(\cos\omega) + 8\pi b_0 B_0 R \cos\omega \quad , \quad R \to \infty \qquad (20b)$$

$$b_0' = \frac{S(1)}{4\pi^2 \sqrt{K_0}} \int_0^\infty \frac{k^2 K_1(k)}{I_1(k)} \, dk \qquad (13c')$$

$$4\pi B_0 = -S(1) + \int_0^1 S(x)dx + \frac{\pi(\gamma+1)}{\sqrt{K_0}} \int_{-\infty}^\infty dx \int_0^\infty \tilde{r}\phi_{0_x}^2(x,\tilde{r})d\tilde{r} \qquad (9b)$$

where ϕ_0 is the solution of (6a) subject to (9a) and

$$\lim_{\tilde{r} \to 0} \tilde{r}\phi_{0_{\tilde{r}}} = S'(x) \quad \text{for} \quad 0 < x < 1 \quad \text{and} \quad \phi_{0_{\tilde{r}}} = 0 \quad \text{for} \quad x > 1 \ .$$

Once the problem P1 is solved, using computational methods such as successive line overrelaxation, the results can be applied to extrapolate to zero model size. In addition, for a fixed K_0, A, and γ, values of K_1 can be determined to achieve $\Delta C_D = 0$ for an interference-free drag simulation. This process is shown schematically in Fig. 4. This result applies to affinely related model geometries for a variety of fineness ratios, wall heights, and blockage ratios.

2.2 CONFINED HIGH ASPECT RATIO CONFIGURATIONS

2.2.1 Asymptotic Representations

The point of departure is the transonic lifting line theory of Ref. 13. This theoretical model treats the case of a high aspect ratio wing in a free

KARMAN GUDERLEY SIMILARITY PARAMETER $K = K_0 + \dfrac{1}{H^3} K_1 + \ldots$

a_r = BLOCKAGE RATIO

Δc_D = PERTURBATION OF MODEL DRAG DUE TO WALLS AND STING

$\dfrac{H \Delta c_D}{a_r}$

INTERFERENCE FREE VALUE

K_1
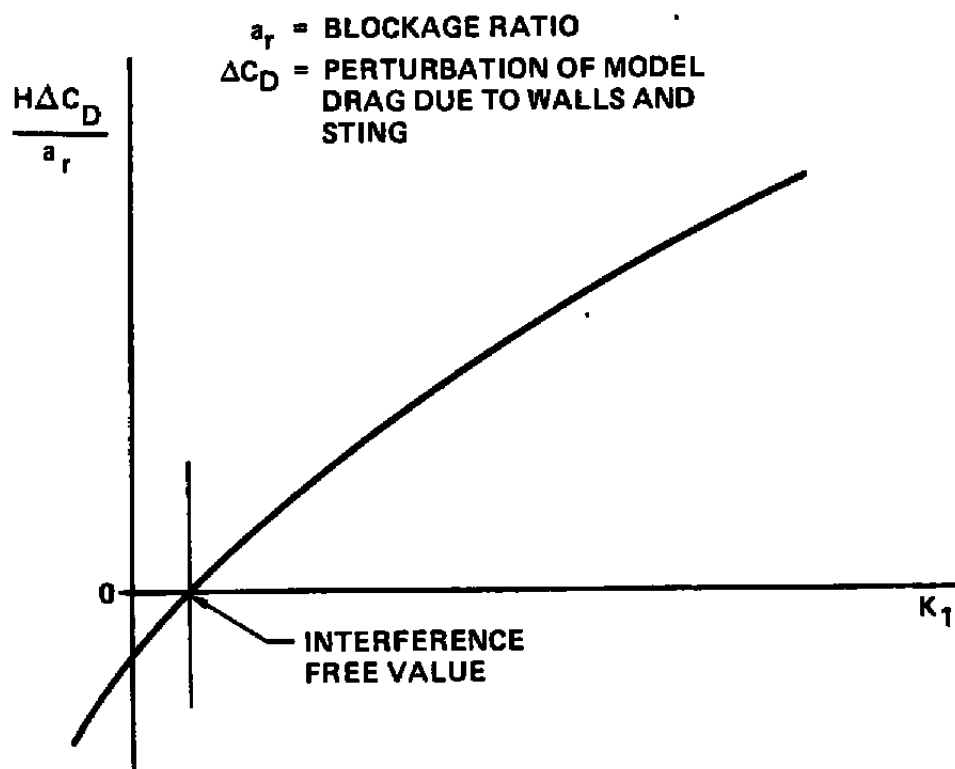
Fig. 4 Schematic of universal plot of interference drag coefficient versus similarity parameter perturbation.

field. Referring to the wing geometry confined within the rectangular tunnel shown in Fig. 5, the free field wing theory applies in a limit in which if δ is a characteristic thickness ratio of a unit chord wing of span b, a transonically scaled aspect ratio parameter, $B = \delta^{1/3}b \to \infty$. This scaling is related to the transverse extent of the wave system which is $O(\delta^{-1/3})$ in a Karman-Guderley (KG) limit involving $\delta \to 0$ to be described. In what follows, if the width of the tunnel is 2h, limits are considered involving B and $H = h\delta^{1/3}$.
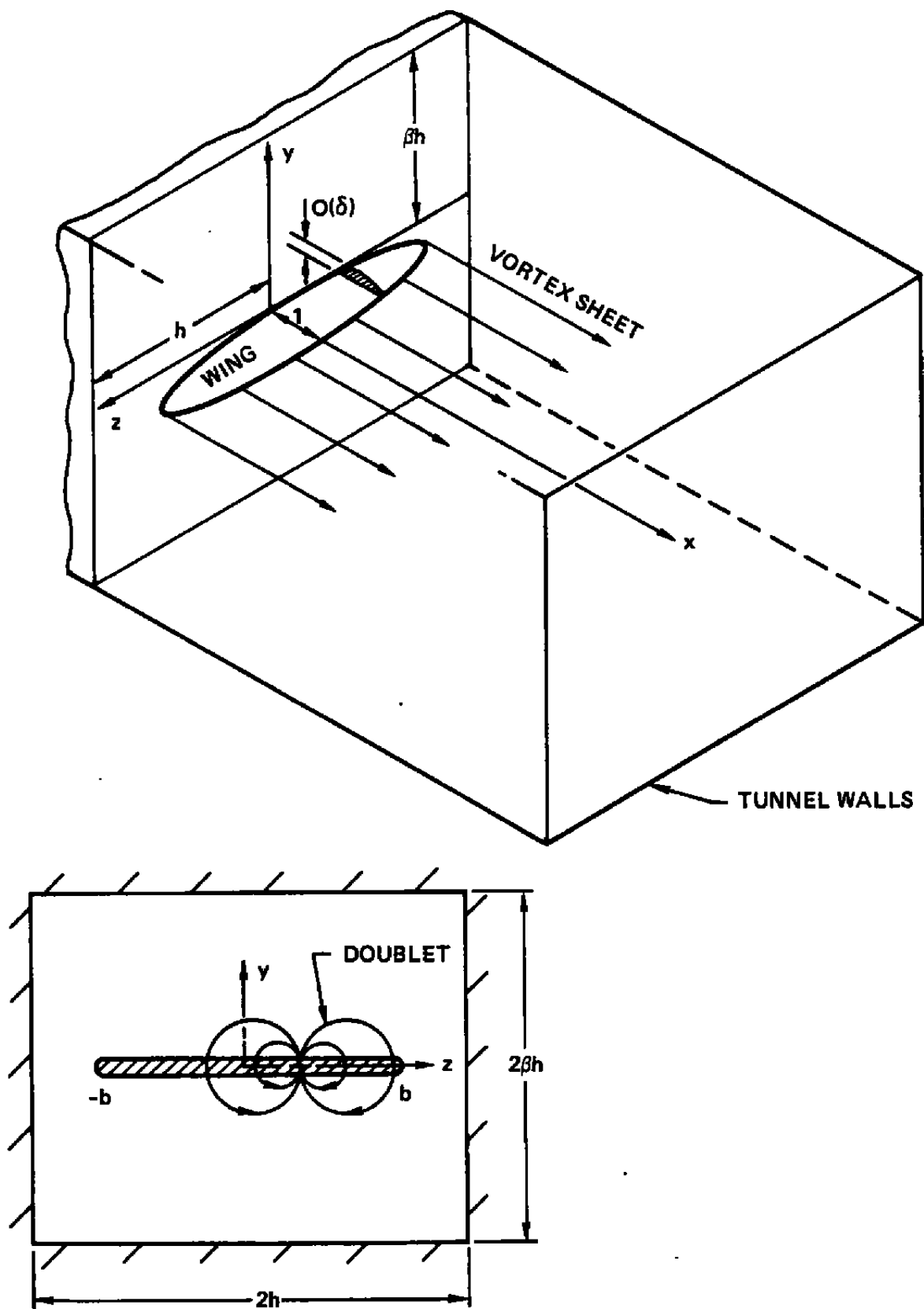
Fig. 5 High aspect ratio wing in rectangular cross section tunnel.

Karman-Guderley Limit

The asymptotic expansion for the velocity potential Φ is

$$\frac{\Phi}{U} = x + \delta^{2/3}\phi(x,\tilde{y},\tilde{z};K,A,H,B) + \cdots \tag{48a}$$

which is valid in the KG limit

$$x,\tilde{y} = \delta^{1/3}y \quad , \quad \tilde{z} = \delta^{1/3}z \quad , \quad K = \frac{1-M_\infty^2}{\delta^{2/3}} \quad , \quad A = \frac{\alpha}{\delta} \text{ fixed as } \delta \to 0 \ . \tag{48b}$$

Substitution of this expansion into the exact equations and boundary conditions leads to the KG problem of transonic lifting surface theory in which the equation of motion

$$\left[K - (\gamma+1)\phi_x\right]\phi_{xx} + \phi_{\tilde{y}\tilde{y}} + \phi_{\tilde{z}\tilde{z}} = 0 \tag{49a}$$

is to be solved subject to the wing and wall boundary conditions

$$\frac{\partial\phi}{\partial\tilde{y}}(x,0,\pm,z) = \frac{\partial F_{u,\ell}}{\partial x}\left(x,\frac{\tilde{z}}{B}\right) - A \tag{49b}$$

$$\frac{\partial\phi}{\partial\tilde{y}}(x,y,\pm H) = \frac{\partial\phi}{\partial\tilde{z}}(x,\pm\beta H,\tilde{z}) = 0 \ , \tag{49c}$$

where the equation of the wing is

$$y = \delta F_{u,\ell}(x,\tilde{z}/B) - A \quad , \quad -B \leqslant z \leqslant B \ .$$

In addition to (49b), the KG formulation also involves wake and far field conditions which will not be considered in this discussion.

Inner Region

For the inner or near field region, the flow is almost two dimensional, with corrections due to the finite aspect ratio and wind-tunnel walls. The asymptotic expansions expressing this structure are

$$\phi(x,\tilde{y},\tilde{z}) = \phi_0(x,\tilde{y};z^*) + \frac{1}{B}\phi_1(x,\tilde{y};z^*) + \cdots \tag{50a}$$

$$K = K_0 + \frac{1}{B}K_1 + \cdots \tag{50b}$$

$$A = A_0 + \frac{1}{B}A_1 + \cdots \ . \tag{50c}$$

The expansion (50a) applies in the limit

$$z^* = \frac{\tilde{z}}{B}, x, \tilde{y}, \frac{H}{B} = \mu \ \text{fixed as} \ \delta \to 0, \ B \to \infty \ \text{independently} \ . \tag{50d}$$

The equations for the approximate quantities associated with (50) are:

$$\left[K_0 - (\gamma+1)\phi_{0_x}\right]\phi_{0_{xx}} + \phi_{0_{\tilde{y}\tilde{y}}} = 0 \tag{51a}$$

$$\left[K_0 - (\gamma+1)\phi_{0_x}\right]\phi_{1_{xx}} - (\gamma+1)\phi_{1_x}\phi_{0_{xx}} + \phi_{1_{\tilde{y}\tilde{y}}} = - K_1\phi_{0_{xx}} \tag{51b}$$

which are to be solved subject to the boundary conditions

$$\left.\frac{\partial\phi_0}{\partial\tilde{y}}\right|_{\tilde{y}=0} = \frac{\partial F_{u,\ell}}{\partial x}(x,\tilde{z}/B) - A_0 \ , \tag{52a}$$

$$\left.\frac{\partial\phi_1}{\partial\tilde{y}}\right|_{y=0} = - A_1 \ . \tag{52b}$$

It is to be noted here that the essential interference problem involves the solution of (51b) which is the wall and aspect ratio correction to the (zero subscript) unconfined two-dimensional near field.

To complete the formulation for the ϕ_1 perturbations, a suitable far field is required. This comes from matching with the outer solution. To dominant order, this represents a bound line vortex shedding its vorticity downstream as an idealization of the wing. If K is sufficiently large, the far field is subsonic and is described by a three-dimensional form of the Prandtl-Glauert equation. In what follows, only this situation will be considered. As contrasted to the free-field case discussed in Ref. 13, the vortex sheet is reflected in the walls.

Outer Expansion

The asymptotic expansion exhibiting the anticipated far field flow features previously discussed is

$$\phi = \varphi_0(x^*,y^*,z^*) + \frac{\log B}{B} \varphi_1(x^*,y^*,z^*) + \frac{1}{B} \varphi_2(x^*,y^*,z^*) + \cdots , \quad (53a)$$

which is valid in the limit

$$x^* = \frac{x}{B} , \quad y^* = \frac{\tilde{y}}{B} , \quad z^* = \frac{\tilde{z}}{B} \text{ fixed as } B \to \infty . \quad (53b)$$

The representation (53a) leads to the hierarchy of equations,

$$K_0\varphi_{0_{x^*x^*}} + \varphi_{0_{y^*y^*}} + \varphi_{0_{z^*z^*}} = 0 \quad (54a)$$

$$K_0\varphi_{1_{x^*x^*}} + \varphi_{1_{y^*y^*}} + \varphi_{1_{z^*z^*}} = 0 \quad (54b)$$

$$K_0\varphi_{2_{x^*x^*}} + \varphi_{2_{y^*y^*}} + \varphi_{2_{z^*z^*}} = (\gamma+1)\varphi_{0_{x^*}}\varphi_{0_{x^*x^*}} - K_1\varphi_{0_{x^*x^*}} , \quad (54c)$$

which are subject to the wall conditions,

$$\frac{\partial \varphi_{0,1,2}}{\partial y^*}\bigg|_{y^*=\pm\beta\mu} = \frac{\partial \varphi_{0,1,2}}{\partial z^*}\bigg|_{z^*=\pm\mu} = 0 \quad , \quad \mu \equiv H/B \; , \tag{55}$$

and appropriate boundedness conditions at $x^* = \infty$, as well as matching with the far field of the inner solution as $x^*, y^* \to 0$. In what follows, results from our first efforts to obtain this behavior are indicated.

Investigations of Inner Limit of Outer Flow

Using Green's theorem, the flow over the wing and its wake can be shown to be the superposition of a surface source, and doublet distribution as well as a nonlinear volume source. The doublet suitable for this representation satisfies the homogeneous Neumann conditions appropriate for the solid walls. If G is the potential of this doublet, dropping star superscripts, and introducing the variable $X = x/\sqrt{K_0}$,

$$\Delta G = \delta'(y)\delta(z-\zeta)\delta(X) \; , \tag{56a}$$

with

$$\frac{\partial G}{\partial y}\bigg|_{y=\beta\mu\equiv\nu} = \frac{\partial G}{\partial z}\bigg|_{z=\mu} = 0 \; . \tag{56b}$$

Introducing the Fourier transform of G, i.e.,

$$\tilde{G} = \frac{1}{\sqrt{2\pi}} \int_{-\infty}^{\infty} e^{ikX} G(X,y,z)dx \; ,$$

(56a) implies

$$\frac{\partial^2 \tilde{G}}{\partial y^2} + \frac{\partial^2 \tilde{G}}{\partial z^2} - k^2\tilde{G} = \frac{1}{\sqrt{2\pi}} \delta'(y)\delta(z-\zeta) \; . \tag{57}$$

2.2.2 Free Field Case

Suppressing the Neumann conditions, (56b), the question of whether the formulation (56a) leads to the free field classical Prandtl lifting line formulas has been answered. This is important in establishing a "datum" term in obtaining a correction to the free field. Denoting G = T for the free field solution, the appropriate solution satisfying (57) with the proper far field decay is

$$\tilde{T} = (2\pi)^{-3/2} \frac{\partial}{\partial y} \left\{ - K_0(kr') \right\} = (2\pi)^{-3/2} \frac{kK_0'(kr')y}{\sqrt{y^2 + (z-\zeta)^2}}$$

where $r' = \sqrt{y^2 + (z-\zeta)^2}$. From inversion and Green's theorem, noting that

$$\int_{-\infty}^{\infty} e^{ikX} K_0(kr)dk = \frac{\pi}{\sqrt{X^2 + r^2}} \, ,$$

the potential, $\varphi_{0,0}$ of a bound vortex shedding a sheet downstream with a shedding strength $\gamma(\zeta)$ is given by the relationship

$$\varphi_{0,0} = \int_{-1}^{1} d\zeta \int_{0}^{\infty} d\xi \gamma(\zeta) T(x,y,z;\xi,\zeta) \, , \tag{58}$$

where

$$T(x,y,z) = - \frac{1}{(2\pi)^2} \int_{-\infty}^{\infty} e^{-ikX} \frac{kK_0'(kr')y}{\sqrt{y^2 + (z-\zeta)^2}} \, dk \, . \tag{59}$$

Thus,

$$\varphi_{0,0} = \frac{1}{4\pi} \int_{-1}^{1} \gamma(\zeta)d\zeta \left\{ 1 + \frac{X}{\sqrt{X^2 + y^2 + (z-\zeta)^2}} \right\} \left\{ \frac{y}{y^2 + (z-\zeta)^2} \right\} \, , \tag{60}$$

which agrees with the Biot-Savart low speed expression for this vortex assemblage.

2.2.3 Confined Case

For finite H, the appropriate expression for $\tilde{G}$ solving the Sturm Liouville problem (57),(56b) is

$$\tilde{G} = \sum_{n=1}^{\infty} \frac{\lambda_n/\nu}{\sqrt{2\pi}\,\beta_n} \frac{\cosh\beta_n(\zeta-\mu)\cosh\beta_n(z+\mu)}{\sinh\beta_n\mu} \sin\lambda_n y \tag{61}$$

where

$$\beta_n = \sqrt{\lambda_n^2 + k^2} \tag{62}$$

$$\lambda_n = \left(n - \frac{1}{2}\right)\frac{\pi}{\nu} . \tag{63}$$

3.0 CONCLUSIONS

Asymptotic theories have been investigated for the treatment of transonic tunnel wall interference. Two limiting cases have been considered. The first which was emphasized in this study involves low aspect ratio shapes where the characteristic lateral dimension of the model is small compared to its length, and the tunnel height is inversely proportional to this lateral dimension. Under these circumstances, key findings are:

1. The wall correction for lift is of higher order than the drag. This contrasts to the two-dimensional case described in Ref. 10 of an airfoil between solid walls for which both corrections are of the same order.

2. A similarity law has been derived for the correction of the drag coefficient. It implies that the change in this quantity (referred to the maximum cross sectional area) due to solid cylindrical wall interference is proportional to the quotient of the blockage ratio and the normalized wall height H.

3. The theory which is applied to the case where the model far field is subsonic gives explicit results for the rate of decay of the model and wall perturbations of the free stream which are not readily accessible from purely computational correction/assessment simulations. Also, it allows extrapolations to zero model size to be made.

4. On the basis of the theory, a perturbation in the Mach number and/or similarity parameter appearing in the theory can be determined to eliminate the tunnel wall perturbation to the drag. As in the lift correction for the two-dimensional case, a universal curve of drag interference-free perturbations to the free stream similarity parameters as a function of the latter can be plotted based on Item 2. This curve, which is a generalization of the transonic area rule, applies to aircraft of differing cross sectional shape variations

in the streamwise direction but with the same longitudinal area progression. The blockage ratio and tunnel height are separated out in this universal variation. The result of universality is that it achieves major computer savings in assessment/correction evaluations.

5. The interference pressure on the body depends only on the streamwise coordinate to dominant order.

The second case considered involves large aspect ratio confined wings. If δ is the wing thickness, b is a span dimension, and h is the tunnel height, both in units of the chord, a limit within transonic small disturbance theory was studied for which $B = b\delta^{1/3}$, $H = h\delta^{1/3} \to \infty$. This process leads to a generalization of lifting line theory considered in Ref. 13. The structure of the flow near the wing (inner solution) and that away from it (outer solution) has been characterized. Near the wing, it retains the two-dimensional character of the free-field case. In the far field, it is the reflection in the walls of a vortex assemblage consisting of a bound vortex perpendicular to the flow shedding trailing vortices. The intensity of the latter is proportional to the spanwise loading. The assemblage induces incidence corrections to the two-dimensional near field. A part of this effect is due to wall corrections not present in the free-field case.

4.0 RECOMMENDATIONS

It is recommended that the theory for slender bodies be extended in several ways. To treat magnetic support systems, Eq. (9a) can be suitably modified by discarding the dominant term $A_0/\underline{R}$. This change gives the appropriate far field doublet rather than source behavior. Equations (12d) and (12e) by appropriate multiplication by k give associated differentiation of the reflected source to obtain the doublet. The same process previously discussed will furnish the asymptotic approximation of these integral representations near the origin, providing the far field in Problem P1. To obtain the correction for pressure boundary conditions and other wall simulations, suitable Green's functions have to be employed in the Green's theorem leading to far field solutions such as (9a). Correspondingly, analogous results replacing Eqs. (12) can be obtained using transform methods and a convolution theorem. For the matching, all of the ideas presented herein for the solid wall, sting supported case will be applicable. In the case of rectangular walls, if β is fixed, it is anticipated that the reflections providing the far field in an analogous problem for P1 will involve elliptic functions.

The large aspect ratio analysis should be completed by determining the inner limit of the outer solution. To obtain this behavior, an integral representation is required for the series (61). One relevant method considers this sum as a residue expansion of a contour integral. From this development, the procedures described herein for the low aspect ratio case can be applied. For the latter, quantitative results should be obtained from a computational solution of the problem formulated in Eqs. (6c), (47), (20b), (13c'), and (9b). Other generalizations besides the ones described previously in this section involve the choked case, and the $K \rightarrow 0$ limit. These are of great practical interest and should also receive attention. The asymptotic methods employed in this report can be advantageously used to treat these situations.

Once these areas have received attention, the combined computational and asymptotic theories should be applied to adaptive walls and incorporation

of viscous effects. Another interesting and important aspect concerns consideration of simplifications of the two variable methods of Refs. 4 and 5 using the tools developed in this effort.

On the basis of the foregoing discussion, the following is a summary list of recommended future follow-on areas to the effort described in this report:

1. Obtain computational solution for transonic slender configurations in circular cross section solid wall tunnels and apply to wind tunnel wall interference assessment and correction procedures.

2. Complete high aspect ratio analysis and develop code.

3. Extend analyses to porous, slotted, and pressure boundary conditions.

4. Extend analyses to other wall cross sections.

5. Treat choked case.

6. Apply theory to adaptive walls.

7. Treat viscous effects.

8. Exploit asymptotic and other theoretical methodology to simplify the two-variable method of Refs. 4 and 5.

5.0 REFERENCES

1. Garner, H.C., Rogers, E.W.E., Acum, W.E.A., and Maskell, E.E., "Subsonic Wind Tunnel Wall Corrections," AGARDograph 109, October 1966.

2. Pindzola, M. and Lo, C.F., "Boundary Interference at Subsonic Speeds in Tunnels with Ventilated Walls," AEDC-TR-69-47 (AD 687440), May 1969.

3. Mokry, M., et al., "Wall Interference on Two-Dimensional Supercritical Airfoils using Wall Pressure Measurements to Determine the Porosity Factors for Tunnel and Ceiling," NRC (Canada) LR-575, February 1974.

4. Kraft, E.M. and Dahm, W.J.A., "Direct Assessment of Wall Interference in a Two-Dimensional Subsonic Wind Tunnel," presented at the AIAA 20th Aerospace Sciences Meeting, Orlando, Florida, January 11-13, 1982.

5. Sickles, W.L. and Kraft, E.M., "Direct Assessment of Wall Interference in a Three-Dimensional Subsonic Wind Tunnel," AEDC-TMR-82-P27.

6. Murman, E.A., "A Correction Method for Transonic Wind Tunnel Wall Interference," AIAA Paper No. 79-1533, 1979.

7. Kemp, W.R., Jr., "Toward the Correctable-Interference Transonic Wind Tunnel," AIAA 9th Aerodynamic Testing Conference, 1976, pp. 31-38.

8. Rizk, M.H., Hafez, M., Murman, E.M., and Lovell, D., "Transonic Wind Tunnel Wall Interference Corrections for Three-Dimensional Models," AIAA Paper No. 82-0588, presented at the AIAA 12th Aerodynamic Testing Conference, Williamsburg, Virginia, March 22-24, 1982.

9. Lo, C.F., "Tunnel Interference Assessment by Boundary Measurements," AIAA J. 16, 4, April 1978.

10. Cole, J.D., Malmuth, N.D., and Zeigler, F., "An Asymptotic Theory of Solid Tunnel Wall Interference on Transonic Airfoils," AIAA Paper No. 82-0933, presented at the AIAA/ASME Joint Thermophysics, Fluids, Plasma, and Heat Transfer Conference, St. Louis, Missouri, June 7-11, 1982.

11. Parker, R.L., Jr. and Erickson, J.C., Jr., "Development of a Three-Dimensional Adaptive-Wall Test Section with Perforated Walls," paper presented at the AGARD meeting on Wall Interference in Wind Tunnels, London, U.K., May 19-20, 1982.

12. Chan, Y.Y., "A Singular Perturbation Analysis of Two-Dimensional Wind Tunnel Interferences," ZAMP 31, 1980, pp. 605-619.

13. Cook, L.P. and Cole, J.D., "Lifting Line Theory for Transonic Flow," SIAM J. Appl. Math. 35, 2, September 1978, pp. 209-228.

14. Van Dyke, M., Perturbation Methods in Fluid Mechanics, The Parabolic Press, Stanford, California, 1975.

15. Cole, J.D., "Studies in Transonic Flow, Transonic Area Rule-Bodies," UCLA Report ENG-7257, August 1972.

APPENDIX A

FAR FIELD CALCULATION OF ϕ_0

To determine the behavior of ϕ_0 for large R, Green's theorem is applied to the region shown in Fig. A1. For this purpose, (6a) is written in a "stretched" coordinate system involving the variable X defined in (8b). This gives Poisson's equation,

$$\Delta\phi_0 = K_0^{-3/2}(\gamma+1)\phi_{0_X}\phi_{0_{XX}} , \tag{A1}$$

where

$$\Delta = \frac{\partial^2}{\partial X^2} + \frac{1}{\tilde{r}}\frac{\partial}{\partial\tilde{r}}\left(\tilde{r}\frac{\partial}{\partial\tilde{r}}\right) .$$
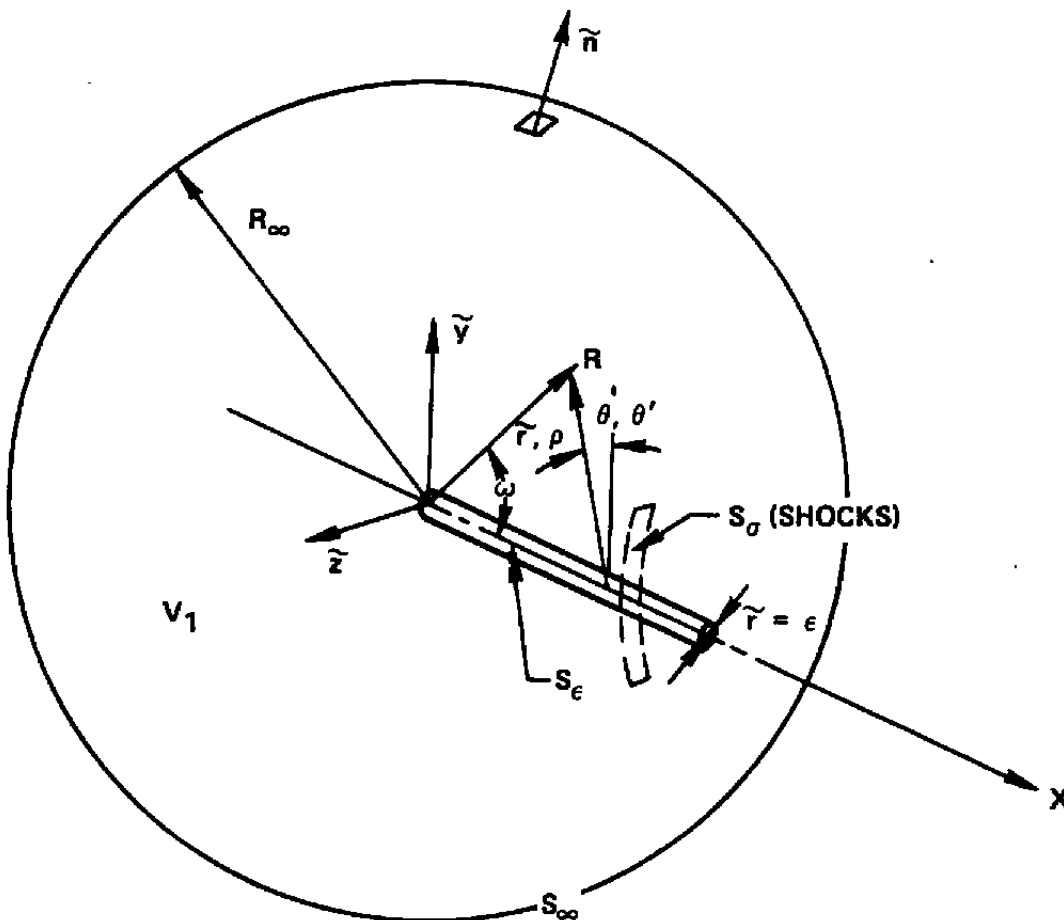

Fig. A1 Region for application of Green's theorem.

In addition, a fundamental solution G is defined with the property that

$$\Delta G = \delta(x-\xi)\,\frac{\delta(\tilde{r}-\rho)}{2\pi\rho}\,\delta(\theta-\theta\text{''})\ .\tag{A2}$$

Green's theorem applied to the region shown in Fig. A1 can be written as

$$\oiint_{S_\epsilon+S_\sigma+S_\infty}\left\{\phi_0\,\frac{\partial G}{\partial n}-G\,\frac{\partial\phi_0}{\partial n}\right\}dS=\iiint_{V_1}\left\{\phi_0\Delta G-G\Delta\phi_0\right\}dV\ ,\tag{A3}$$

where n denotes differentiation in the direction of the outward normal to the region V_1. In (A3), the left hand side represents an integration over the surfaces S_ϵ, S_σ, and S_∞. The surface S_ϵ is a slender cylinder of radius $\tilde{r}=\epsilon$ with the X axis as its axis of symmetry. The surface S_σ is the total area of the shocks, and S_∞ is an infinitely large sphere.

The right hand side of (A3) represents a volume integration over V_1. On the basis of (A2),

$$G=-\frac{1}{4\pi}\cdot\frac{1}{\sqrt{(X-\xi)^2+\tilde{r}^2-2\tilde{r}\rho\,\cos(\theta-\theta')+\rho^2}}\tag{A4a}$$

$$\frac{\partial G}{\partial\rho}=\frac{1}{4\pi}\cdot\frac{\rho-r\,\cos(\theta-\theta')}{[(X-\xi)^2+\tilde{r}^2-2\tilde{r}\rho\,\cos(\theta-\theta')+\rho^2]^{3/2}}\ .\tag{A4b}$$

For a sting support, it is anticipated that ϕ_0 will behave dominantly in a subsonic far field like an unconfined source, i.e., $\phi_0\cong-\frac{1}{4\pi R}$. From (A3) and this assumption, the contribution from S_∞ is $O(R^{-1})$ as $R\rightarrow\infty$ and therefore vanishes. For the magnetic suspension case, the doublet behavior, $\phi_0=O(R^{-2})$ is expected and again the contribution from S_∞ vanishes. The integral on the shock surfaces S_σ also disappears. This can be demonstrated in the same manner as in the two-dimensional case by

44

integration by parts of the right hand side of (A3). Combination of boundary terms from the partial integration and the S_σ integral nullifies the shock contribution by the shock relations.

Implementing this procedure, (A3) can be written as

$$I_1 + I_2 = I_3 + I_4 + I_\sigma \qquad (A5)$$

where

$$I_1 = \iint\limits_{S_\epsilon} \phi_0 \frac{\partial G}{\partial n} \, dS \qquad (A6a)$$

$$I_2 = - \iint\limits_{S_\epsilon} G \frac{\partial \phi_0}{\partial n} \, dS \qquad (A6b)$$

$$I_3 = \iiint\limits_{V_1} \phi_0 \Delta G \, dV \qquad (A6c)$$

$$I_4 = - \iiint\limits_{V_1} G \Delta \phi_0 \, dV \qquad (A6d)$$

$$I_\sigma = - \iint\limits_{S_\sigma} \left\{ \phi_0 \frac{\partial G}{\partial n} - G \frac{\partial \phi_0}{\partial n} \right\} dS \ . \qquad (A6e)$$

On the basis of anticipated matching with the Axis Layer as described in connection with (24c),

$$\phi_0 \simeq \frac{S'(x)}{2\pi} \ln \tilde{r} + g(x) \quad \text{as} \quad \tilde{r} \to 0 \ . \qquad (A7)$$

Approximating G and $\frac{\partial G}{\partial \rho}$ for $\rho \to 0$, and use of (A7) gives

$$I_1 \simeq \int_0^\infty d\xi \int_0^{2\pi} \left[\frac{S'(\xi)}{2\pi} \ell n \varepsilon + g(\xi) \right] \frac{\varepsilon(-r \cos(\theta-\theta') + \cdots)d\theta'}{4\pi[(X-\xi)^2 + r^2 - 0(\varepsilon)]^{3/2}}$$

$$= 0(\varepsilon \, \ell n \varepsilon) \quad \text{as} \quad \varepsilon \to 0 \ . \tag{A8}$$

In a similar manner, noting that $S'(x) = 0$ for $x > 1$,

$$I_2 \simeq -\frac{1}{4\pi} \int_0^1 \frac{S'(\xi)d\xi}{\sqrt{R^2 - 2\xi R \cos\omega + \xi^2}} = -\frac{1}{4\pi} \sum_{n=0}^\infty \frac{P_n(\cos\omega)}{R^{n+1}} \int_0^1 \xi^n S'(\xi)d\xi \ ,$$

from expanding the denominator in Legendre polynomials and termwise integration.

On integration by parts and letting $R \to \infty$, this becomes

$$I_2 = \frac{S(1)}{4\pi R} + \left\{ S(1) - \int_0^1 S(\xi)d\xi \right\} \frac{\cos\omega}{4\pi R^2} + \left\{ S(1) - 2 \int_0^1 \xi S(\xi)d\xi \right\} \frac{P_2(\cos\omega)}{4\pi R^3} + 0(R^{-4})$$

$$\tag{A9}$$

where the factor in the second braces representing the strength of the quadrupole contributes to the quantity $\underline{A}$ in (9a).

By (A2), (A6c) gives

$$I_3 = \phi_0 \ . \tag{A10}$$

From (A1), (A6d) becomes

$$I_4 = \frac{\gamma+1}{K_0^{3/2}} \iiint_{V_1} \left(\phi_{0_\xi} \phi_{0_{\xi\xi}} \right) G dV \ . \tag{A11}$$

Integrating (A11) by parts, combining the boundary terms with those in I_σ, applying the shock relations, and collecting the results for I_1, I_2, and I_3 gives the first two terms of (9a). These are the first two spherical

harmonic solutions of (A1), assuming the response to the nonlinear forcing term is negligible. The higher order terms include the response to this forcing term. For this purpose, the forcing term is evaluated for large R, from the dominant representation of ϕ_0.

Accordingly,

$$\phi_{0_X}\phi_{0_{XX}} = -\frac{2A_0^2}{R^5}P_1(\cos\omega)P_2(\cos\omega) - \frac{A_0B_0}{R^6}(6P_1P_3 + P_2^2) + \cdots , \qquad (A12)$$

where from (9a),

$$A_0 = \underline{A}_0/\sqrt{K_0} \quad , \quad B_0 = \underline{B}_0/K_0 ,$$

and $P_n(\cos\omega)$ is a Legendre polynomial of order n. The products of the Legendre polynomials can be expressed as a sum of them (Ref. A1). This fact facilitates the determination of the particular solutions. In particular, denoting $u = \cos\omega$,

$$P_1(u)P_2(u) = \frac{3u^3 - u}{2} = \frac{3P_3 + 2P_1}{5} . \qquad (A13)$$

To obtain the particular solutions, (A1) is written in spherical coordinates, and the method of separation of variables is used. Considering the response to a typical forcing term in (A12), using (A13), this gives

$$\Delta\phi_0 = \frac{1}{R^2}\frac{\partial}{\partial R}\left(R^2\frac{\partial\phi_0}{\partial R}\right) + \frac{1}{R^2\sin\omega}\frac{\partial}{\partial\omega}\left(\sin\omega\frac{\partial\phi_0}{\partial\omega}\right) = \frac{P_n(\cos\omega)}{R^5} ,$$

[A1] Gradshteyn, I.S. and Ryzhik, I.M., Tables of Integrals, Series and Products, Corrected and Enlarged Edition, Academic Press, New York, 1980, Eq. (8915,5), p. 1026.

In which

$$\phi_0 = \mathscr{R}(R)T(\omega) . \tag{A14}$$

If $T = P_n(\cos\omega)$,

$$\mathscr{R} = \frac{R^{-3}}{6 - n(n+1)} . \tag{A15}$$

The special case, $n=2$ in (A15) leads to irrelevant logarithmic solutions. Others are of higher order and are indicated by the 0 symbol in (9a). These are unimportant for the matching discussion in this report. On the basis of this analysis, the forcing term response particular solution to the dominant source term of ϕ_0, $\phi_0^{(p)}$ is

$$\phi_0^{(p)} = \frac{S^2(1)(\gamma+1)}{16\pi^2 K_0 [x^2 + K_0\tilde{r}^2]^{3/2}} \left\{ \cos3\omega + \frac{2}{5} \cos\omega \right\} , \tag{A16}$$

and leads to (9a).

In connection with this derivation, it should be noted that in (A8) the lift effect is associated with a doublet term (not shown), $\sim \cos\theta'/\varepsilon$, that is in the bracketed factor in the integrand. This term is higher order in δ in the limit (4) as can be inferred from matching of the Axis and Central Layers. Therefore, it has been neglected in this analysis.

APPENDIX B

DERIVATION OF DOMINANT APPROXIMATION FOR
WALL LAYER φ_0 GIVEN BY EQ. (12a)

The singular behavior

$$\varphi_0 \doteq \frac{S(1)}{\sqrt{K_0}} \left\{ -\frac{1}{4\pi R^+} + \cdots \right\} \quad \text{as} \quad R^+ \to 0 , \tag{B1}$$

$$R^+ = R/H ,$$

by virtue of the need to match with ϕ_0, is anticipated. Accordingly, (11a) can be rewritten as

$$\Delta\varphi_0 = \frac{S(1)}{\sqrt{K_0}} \delta(X^+) \frac{\delta^+(r^+)}{2\pi r^{+2}} , \tag{B2}$$

where $\int_0^\infty \delta^+(r)dr = 1$. The appropriate boundary condition associated with solid walls is

$$\left. \frac{\partial\varphi_0}{\partial r^+} \right|_{r^+=1} = 0 . \tag{B3}$$

Applying the divergence theorem to the region bounded by a cylinder consisting of the curved surfaces, $r^+=1$, and the flat faces $X \to \infty$, (B2) and (B3) imply that

$$\varphi_0 \simeq \frac{S(1)}{\sqrt{K_0}} \frac{X^+}{2\pi} \text{sgn } X^+ . \tag{B4}$$

To solve the boundary value problem embodied in (B2) and (B3), the exponential Fourier transform is used. For the purpose of obtaining convergent integrals, the property (B4) is utilized to define a regularized version of φ_0 denoted by M for which

$$\varphi_0 = \frac{S(1)}{\sqrt{K_0}} \left\{ \frac{X^{\dagger}}{2\pi} \, \text{sgn} \, X^{\dagger} + M \right\} . \tag{B5}$$

Accordingly,

$$\Delta M = \left\{ \frac{\delta^{+}(r^{\dagger})}{2\pi r^{\dagger}} - \frac{1}{\pi} \right\} \delta(X) . \tag{B6}$$

With the following exponential transform pair,

$$\bar{M} = \int_{-\infty}^{\infty} e^{-ikX} M dX \tag{B7}$$

$$M = \frac{1}{2\pi} \int_{-\infty}^{\infty} e^{ikX} \bar{M} dk , \tag{B8}$$

the subsidiary equations for $\bar{M}$ become:

$$\frac{1}{r} \frac{d}{dr} \left(r \frac{d\bar{M}}{dr} \right) - k^2 \bar{M} = \frac{\delta^{+}(r)}{2\pi r} - \frac{1}{\pi} . \tag{B9}$$

The first forcing term on dropping the daggers on r and X can be eliminated and replaced by the boundary condition

$$\lim_{r \to 0} r \frac{d\bar{M}}{dr} = \frac{1}{2\pi} . \tag{B10}$$

The other boundary condition is

$$\left.\frac{d\bar{M}}{dr}\right|_{r=1} = 0 \ .$$

(B11)

The solution of the boundary value problem is

$$M = \frac{1}{2\pi} \int_{-\infty}^{\infty} e^{ikX} \left\{ \left[\frac{K_0'(k)I_0(kr) - K_0(kr)I_0'(k)}{2\pi I_0'(k)} \right] + \frac{1}{\pi k^2} \right\} dk$$

(B12)

where the effect of the last term regularizer in the braces eliminates the double pole at the origin. Since $I_0'(z) = I_1(z)$ has only pure imaginary simple zeroes, the appropriate inversion contour is a large semicircle with its base along the real axis. For $|k| \to \infty$, the square bracket term is $0\left(\frac{e^{-|\mu|r - \tau X}}{\sqrt{|k|}} \right)$, where $k = \mu + i\tau$. Accordingly, the semicircle is in the upper half plane for $X > 0$, and in the lower for $X < 0$. The zeroes of I_0' are at $k = \pm i\lambda_n$, $n = 1, 2, \cdots$. λ_n is the solution of the equation

$$J_1(\lambda_n) = 0 \ .$$

(B13)

On summing the residues at the poles corresponding to these zeroes, we obtain

$$M = \frac{1}{2\pi} \sum_n \frac{e^{-\lambda_n |X|}}{\lambda_n} \frac{J_0(\lambda_n r)}{[J_0(\lambda_n)]^2}$$

(B14)

where the Wronskian relation

$$J_0(\lambda_n)Y_0'(\lambda_n) - Y_0(\lambda_n)J_0'(\lambda_n) = \frac{2}{\pi\lambda_n}$$

and (B13) have been utilized in (B14), which can also be derived by eigenfunction expansions.

Equations (12c)-(12e) follow from (B12) and the properties of the modified Bessel functions, upon restoring the daggers and noting that (B9) admits solutions for positive and negative values of k.

APPENDIX C

DERIVATION OF BEHAVIOR OF φ_0 NEAR ORIGIN $R^\dagger = 0$ GIVEN BY EQ. (13a)

To obtain the required representation, (12d) and (12e) will be considered. Now, M_0 can be evaluated exactly from a table of Fourier transforms to give

$$M_0 = -\frac{1}{4\pi R^\dagger} \,.$$ (C1)

This is precisely the source behavior desired for matching.

One candidate method of evaluating M_1 involves expansion of the integrand near the origin. This leads to divergent integrals. To avoid this difficulty, the derivatives of M_1 with respect to $r^\dagger$ and $X^\dagger$ are considered using the same procedure. Accordingly, on dropping the daggers,

$$\frac{\partial M_1}{\partial r} = -\int_0^\infty \frac{k \cos kX}{2I_1(k)} K_1(k) I_1(kr) dk$$

$$\approx -r\overline{I_1} \,,$$ (C2a)

on expanding the trigonometric factor cos kX and integrating term by term with

$$\overline{I_1} = \int_0^\infty \frac{k^2 K_1(k)}{I_1(k)} dk \,.$$ (C2b)

Since the integrand of $\overline{I_1}$ is bounded at the origin and $O(k^2 e^{-2k})$ as $k \to \infty$, it is evident that $\overline{I_1}$ converges.

Moreover,

$$\frac{\partial M_1}{\partial X} = - \int_0^\infty k \sin kX \left\{ \frac{-K_1(k)}{2I_1(k)} \right\} dk - \int_0^\infty \frac{\sin kX}{k} dk \; . \tag{C3}$$

Again, expanding the trigonometric factor and recognizing that the last integral is well known, and can be evaluated by Cauchy's theorem as $\frac{\pi}{2}$ sgn X, $\frac{\partial M_1}{\partial X}$ is given as

$$\frac{\partial M_1}{\partial X} = \frac{X}{2} \overline{I_1} - \frac{\pi}{2} \text{sgn } X \; . \tag{C4}$$

Since

$$M_1(0,0) = \frac{1}{\pi^2} \int_0^\infty \left\{ \frac{1}{k^2} - \frac{K_1(k)I_0(kr^\dagger)}{2I_1(k)} \right\} dk \; , \tag{C5}$$

which is itself a convergent integral, utilization of (C2), (C4), and (C5) with (12a) leads to (13). This result could also have been obtained from a Taylor's expansion of M_1 near the origin. It is interesting to note in this connection that the second term in (C4) leads to cancellation with the first term in (12a) as $R^\dagger \to 0$.

NOMENCLATURE

A	Angle of attack parameter
$\underline{A}$	Constant appearing in (9a)
A_0, A_1	Approximations in angle of attack parameter expansion (5d)
$\underline{A_0}$	Constant appearing in (9a)
a_0	Constant appearing in (13b)
a_0'	Constant defined in (22b)
a_r	Blockage ratio
B	Reduced span $= \delta^{1/3}b$, body function
$\underline{B_0}$	Constant appearing in (9a)
$\underline{b}$	Span
b_0	Constant defined in (13c)
b_0'	Constant defined after Eq. (20b)
$\underline{C_0}$	Constant appearing in (9a)
C_D	Drag coefficient
ΔC_D	Wall interference effect on drag coefficient
C_p	Pressure coefficient
c	Chord
D	Drag force
F	Body shape function in (1)
G	Green's function
g	Function defined in (44)
$g_0^{*(n)}$	Functions appearing in (26a)
$g_n(x)$	Functions appearing in (30)

H	Reduced tunnel radius in (4), and tunnel height defined before (48a)
h	Tunnel dimension in units of chord
I_n	Modified Bessel function and designation of integrals in (A5)
I_σ	Integral in (A5)
K	Transonic similarity parameter in Eq. (4)
K_n	Modified Bessel function
K_0, K_1	Dominant two terms in asymptotic expansion for K (5c)
k	Fourier transform variable of integration
M_0, M_1	Portions of φ_0 solution in (12a)
$P_n(\cos\omega)$	Legendre polynomial
q	Dynamic pressure
R	Reduced polar radius in (8b)
$\underline{R}$	Scaled polar radius in (8a)
$R^\dagger$	Reduced polar radius = R/H
R_η	Intermediate variable R/η(H)
R_ζ	Intermediate variable R/ζ(H)
$\mathscr{R}$	Function of R in separation of variables solution (A15)
r	Cylindrical coordinate
$\tilde{r}$	δr
$r^\dagger$	$\tilde{r}$/H
r^*	r/δ
S(x)	Reduced cross sectional area
S_ϵ	Area in Fig. A1
S_σ	Area on shock in Fig. A1
S_∞	Area at infinity in Fig. A1

$\mathscr{P}(x)$	Source strength = $S'(x)/2\pi$
$T(\omega)$	Function of ω in separation of variables solution (A15)
U	Freestream velocity
u	$\cos\omega$
$\dot{V}_1$	Volume of region in Fig. A1
X	$x/\sqrt{K_0}$
$X^\dagger$	X/H
$\bar{x},\bar{y},\bar{z}$	Dimensional Cartesian coordinates
x,y,z	Nondimensional Cartesian coordinates
$\tilde{y},\tilde{z}$	δy, δz, respectively
$y^\dagger,z^\dagger$	$\tilde{y}/H$, $\tilde{z}/H$, respectively
x^*	x/B
y^*,z^*	$\tilde{y}/\delta$, $\tilde{z}/\delta$ or $\tilde{y}/B$, $\tilde{z}/B$
α	Angle of attack
β	Aspect ratio of rectangular tunnel cross section defined in Fig. 5
β_n	$\sqrt{\lambda_n^2 + k^2}$
ε	Radius of internal cylindrical boundary S_ε in Fig. A1
γ	Specific heat ratio
δ	Thickness ratio, characteristic flow deflection
$\delta(x)$	Delta function
Δ	Laplacian operator
ε_n	Gauge function appearing in Wall Layer expansion (10)
ξ,η,ζ	Dummy Cartesian coordinates
θ	Azimuth angle in spherical coordinates, cylindrical coordinates
θ'	Dummy variable for θ

κ_n — Gauge function appearing in angle of attack parameter expansion (5d)

λ_n — Eigenvalue appearing in (63) and (B13)

μ — H/B in (55)

μ_n — Gauge functions appearing in Central Layer expansion (5a)

ν_n — Gauge functions appearing in similarity parameter expansion (5c)

ν — $\beta\mu$

ω — Polar angle in spherical polar coordinates

ρ — Dummy variable for $\tilde{r}$

φ_n — Approximations for perturbation potential appearing in Wall Layer expansion (10) and (53a)

ϕ — Perturbation potential defined in (48a)

ϕ_n — Perturbation potential approximations in Central Layer representation (5a) and (50a)

ϕ_n^* — Perturbation potential approximations in Axis Layer representation (23a)

Φ — Velocity potential

τ_n — Gauge function appearing in (23a)

Subscripts

B — On body

ℓ — Lower surface

u — Upper surface

Special Symbols

Overbar
Tilde } Denote Fourier transform